RSC Advances

This is an *Accepted Manuscript*, which has been through the Royal Society of Chemistry peer review process and has been accepted for publication.

Accepted Manuscripts are published online shortly after acceptance, before technical editing, formatting and proof reading. Using this free service, authors can make their results available to the community, in citable form, before we publish the edited article. This *Accepted Manuscript* will be replaced by the edited, formatted and paginated article as soon as this is available.

You can find more information about *Accepted Manuscripts* in the Information for Authors.

Please note that technical editing may introduce minor changes to the text and/or graphics, which may alter content. The journal's standard Terms & Conditions and the Ethical guidelines still apply. In no event shall the Royal Society of Chemistry be held responsible for any errors or omissions in this *Accepted Manuscript* or any consequences arising from the use of any information it contains.

ROYAL SOCIETY OF CHEMISTRY

www.rsc.org/advances

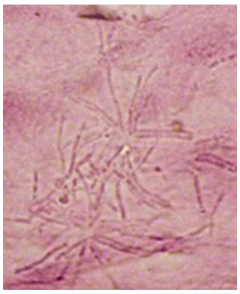

Electrospinning fibrous scaffold was used in the in situ remediation of rabbits' corneal stroma.

RSC Advances Accepted Manuscript

In Situ Induction Growth of the Corneal Stroma Cells in Uniaxially Aligned Composite Fibrous Scaffold

Cong Zhang[a], Jihong Wen[*b], Jing Yan[c], Yanbing Kao[d], Zhiqiang Ni[e], Xuejun Cui[a], Hongyan Wang[*a]

[a] College of Chemistry, Jilin University, Changchun 130012, P. R. China

[b] Department of Jilin University, First Clinical Hospital of Bethune Medical,Changchun 130012, P. R. China

[c] Department of Chemistry and Biochemistry Nanocenter,University of South Carolina, Columbia ,South Carolina 29208

[d] Clinic College of Medicine, Jilin University, Changchun 130012, P. R.

[e] Department of Tumor Biological Therapy Jilin Province People's Hospital, Changchun 130012, P. R. China

Tel: +86-431-85168470

Fax: +86-431-85175863

E-mail: wang_hy@jlu.edu.cn

RSC Advances Accepted Manuscript

Abstract

Uniaxially aligned composite fibrous scaffolds of gelatin and poly-L-lactic acid (PLLA) were fabricated by electrospinning and the scaffolds were implanted into the corneal stroma layer of New Zealand white rabbits (NZWRs) to observe the *in situ* induction growth of the stroma cells. The effects on cell growing were evaluated by both apparent observation and pathological analysis. It was demonstrated that the scaffolds had good compatibility with corneal tissues and was nontoxic by observing the changes of structure and physiological activity of the corneal tissue around the scaffolds with slit lamp and vivo confocal images. The in vivo confocal images of scaffolds that implanted into the eyes of NZWRs showed the process of the cells' ingrowth and the tissue regeneration, which indicated that the uniaxially aligned fibers could induce the polarized ingrowth of keratocytes and this may provide basis for clinical application of *in situ* repair of corneal stroma.

Key Words: electrospinning, aligned fibrous scaffolds, corneal stroma, *in situ* repair, tissue engineering

RSC Advances Accepted Manuscript

1. Introduction

Cornea is a transparency tissue on the surface of eyeball, which plays important roles in both protecting the eyes and the formation of vision. So the health of cornea is the precondition of normal vision.[1,2] Corneal disease has already become the second eye disease leading to blindness in the world.[3,4] The shortage of donors is a major problem in the treatment of corneal grafts.[5,6] The corneal tissue engineering provides a new approach for corneal repair.[7,8] However, the greatest challenge of corneal tissue engineering is how to realize the special physiological function of cornea.[9] And the special physiological structure of corneal stroma is the key to maintaining its function.[10,11] Human cornea stroma is about 500μm thick, and its extracellular matrix is consist of more than 200 thin layers of parallel and staggered collagen fibers with uniform diameter of 30nm.[12,13]

Although gel and sponge with disordered structure composed by collagen or other biological materials have realized the reconstruction of corneal tissue in vitro,[14] but at present none of these tissue engineering corneas has the above-mentioned ordered structure in the reconstructed stroma.[15] Researches have shown that,[16,17] compared with randomly oriented fibrous scaffold, the uniaxially aligned scaffold of gelatin and PLLA, which has the same parallel arrangement with normal corneal cells, can induce the growth of matrix cells along the fibers more greatly. At the same time, this scaffold allows corneal cells to grow into it and form three-dimensional structure. Thus it is speculated that this scaffold can provide physical support and induce the directional growth of corneal cells.

RSC Advances Accepted Manuscript

On the basis of previous work,[16, 17] the uniaxially aligned composite fibrous membrane of gelatin and PLLA was prepared and used to induce the *in situ* growth of autologous corneal stroma cells of NZWRs.

2. Experimental Section

2.1. Materials

Gelatin (type A, from porcine skin, Sigma) and poly-L-lactic acid (PLLA, Mw=300,000, from Shandong Institute of Medical Appliances, People's Republic of China) were used as materials for electrospinning. 1, 1, 1, 3, 3, 3-Hexafluoro-2-propa-nol (HFIP) and N, N-dimethylformamide (DMF, from Atoz Fine Chemicals) were used as the solvents for electrospinning. Ethanol (EtOH) and dimethyl sulfoxide (DMSO, also from Atoz Fine Chemicals) were used as received. Xylazine hydrocloride injection and tetracaine hydrochloride injection (from animal experimental center of Norman Bethune College Of Medicine, Jilin University) were used as anaesthetic. 3,3'-diaminobenzidine color developing reagent kit (DBA, Shanghai Sangon Biotech Company) was used for immunohistochemical staining. Experimental animals were NZWRs purchased from animal experimental center of Norman Bethune College Of Medicine, Jilin University. The sterile surgical suture MANI10-0 was imported from Japan. All the other chemicals and agents were analytically pure.

RSC Advances Accepted Manuscript

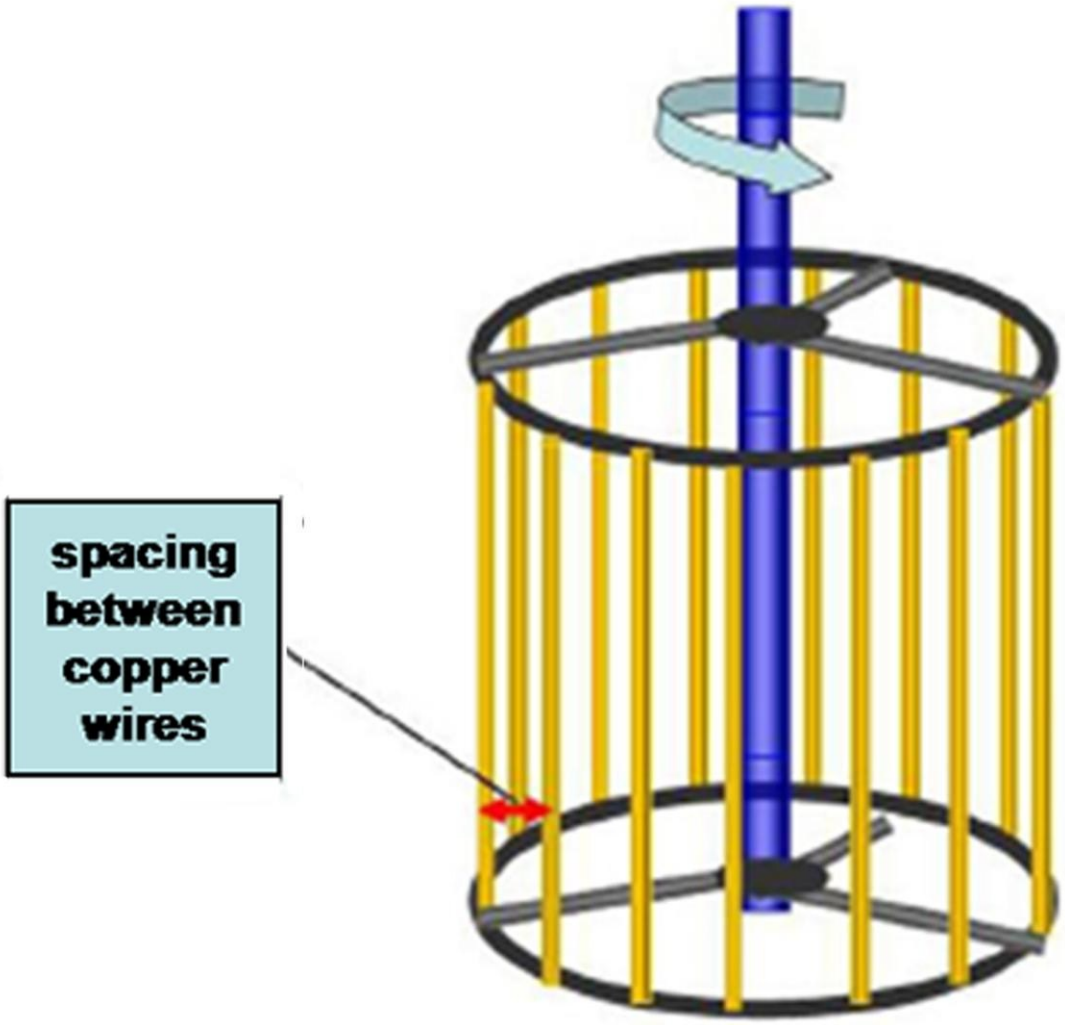

Figure 1. The electrospinning receiver of aligned nanofibers - rotating copper wire drum.

2.2. Preparation of Aligned Gelatin/PLLA Fibrous Scaffold

A certain amount of gelatin and PLLA -G70P30 (mass ratio of gelatin to PLLA was 70:30) was successively dissolved in the mixed solvent of HFIP and DMF (volume ratio of HFIP to DMF was 4:1) to prepare 10% of the mixture polymer solution. The polymer solution was placed into a 5mL syringe with a needle of 0.4 mm inner diameter and was pumped by a syringe pump at a rate of 30μL/min. The electrospinning voltage

RSC Advances Accepted Manuscript

was 15 kV, the distance of tip-to-collector was 18 cm and the ambient humidity was controlled at 60-70%. The copper wire drum (Figure 1) was used as a receiver for aligned composite fibrous scaffold. Then the aligned composite fibrous was placed into the vacuum drying oven to remove the residuary solvent.

2.3. Analytical Methods

2.3.1. Morphology of aligned composite fibrous scaffold.

The morphology of the electrospun aligned gelatin/PLLA fibrous membrane was characterized by scanning electron microscopy (SEM, Shimadzu SSX-550) at an accelerating voltage of 3 kV. Average fiber diameter was measured with the software of Photoshop.

2.3.2. Damage model and implantation experiment.

The fibrous membranes were cut into circular discs of 6 mm in diameter and 0.5mm in thickness and disinfected with 75% (volume fraction) ethanol for 30 min. Then the cut scaffolds were washed with sterile Hank's solution for 3 times, immersed in serum-free medium DMEM and then placed into refrigerator at 4 °C for overnight. These operations were performed in a super clean bench. The disinfected scaffolds were washed by sterile phosphate buffer solution to wipe off the medium before implantation.

18 healthy NZWRs were generally anesthetized with xylazine hydrochloride

RSC Advances Accepted Manuscript

(application amount: 0.4 mg/Kg) by intramuscular injection, and then locally anesthetized with 1% tetracaine hydrochloride injection. A slight mark was drilled on the cornea by a trephine with a diameter of 7.5mm and an incision about 2cm long was opened beside the drilled mark. After that, a matrix vesicle of 6.5 mm in diameter was made in the middle of corneal stroma by iris separator, and on the vesicle, an artificial minimally invasive wound was created. Then the disinfected scaffolds were implanted into the vesicle, and spread evenly. Finally the incision was sewed with No.10 sterile surgical suture, and the operation was completed. All animal handling procedures conformed to the National Institutes of Health Guide for the Care and Use of Laboratory Animals.

2.3.3. Clinical characterization

18 rabbits were divided into 6 groups and the samples of clinical characterization were respectively taken from the rabbits after the operation for 0 days, 2, 6, 12, 24 and 32 weeks. The clinical phenomenon was observed by slit lamp, anterior segment optical coherence tomography (OCT) and intravital confocal microscopy through focusing (CMTF).

After the operation, the experimental eyes were observed by slit lamp (HPG100, OLYMPUS, Japan) after 0 days,2, 6, 12, 24 and 32 weeks respectively to record the corneal transparency and the growth of new blood vessels.

RSC Advances Accepted Manuscript

The anterior segment OCT (made in German, Carl Zeiss company) was used to estimate the degradation of the fibrous scaffold and the ingrowth rate of the cells and to measure the thickness of the cornea. The distance between the instrument and experimental eye was adjusted until a vertical white stripe appeared in the center of the cornea, then real-time scanning was made. At last the images were analyzed to measure the corneal curvature and thickness.

The phenotype and density of the cells were inspected by the intravital CMTF (made in Japan NIDEK company, the fourth generation). The magnification was set to 1000×, the scanning range was 340×255 μm, and the scanning thickness was about 700 μm. 350 images were got in every scan. The surface of experimental corneal was perpendicular and close to the objective lends, and cells of different layers were scanned and recorded images. Then the NAVIS software was used in the image analyzation to count the cell density of epithelium, anterior stroma, posterior stroma and endothelium.

2.3.4. Pathology characterization

Samples were taken at 2, 6, 12, 24 and 32 weeks after the operation respectively and were immersed in 4% paraformaldehyde solvent quickly to fix the cells, then the samples were stained by conventional HE and immumohistochemical methods. In the immumohistochemical staining of the vimentin in corneal stroma cytoplasm, the First Ab

RSC Advances Accepted Manuscript

was rabbit mono-clonal anti-vimentin, and the Second Ab was goat anti-rabbit IgG-HRP. In the immumohistochemical staining of the vimentin in corneal epithelial cytoplasm, the First Ab was rabbit monoclonal anti-keratin K3/K76 antibody, and the Second Ab was goat anti-rabbit IgG- HRP. The concentrations of First Abs and Second Abs were respectively 1:200 and 1:400.Then the samples were observed and analyzed by optical microscope and Scopephoto software.

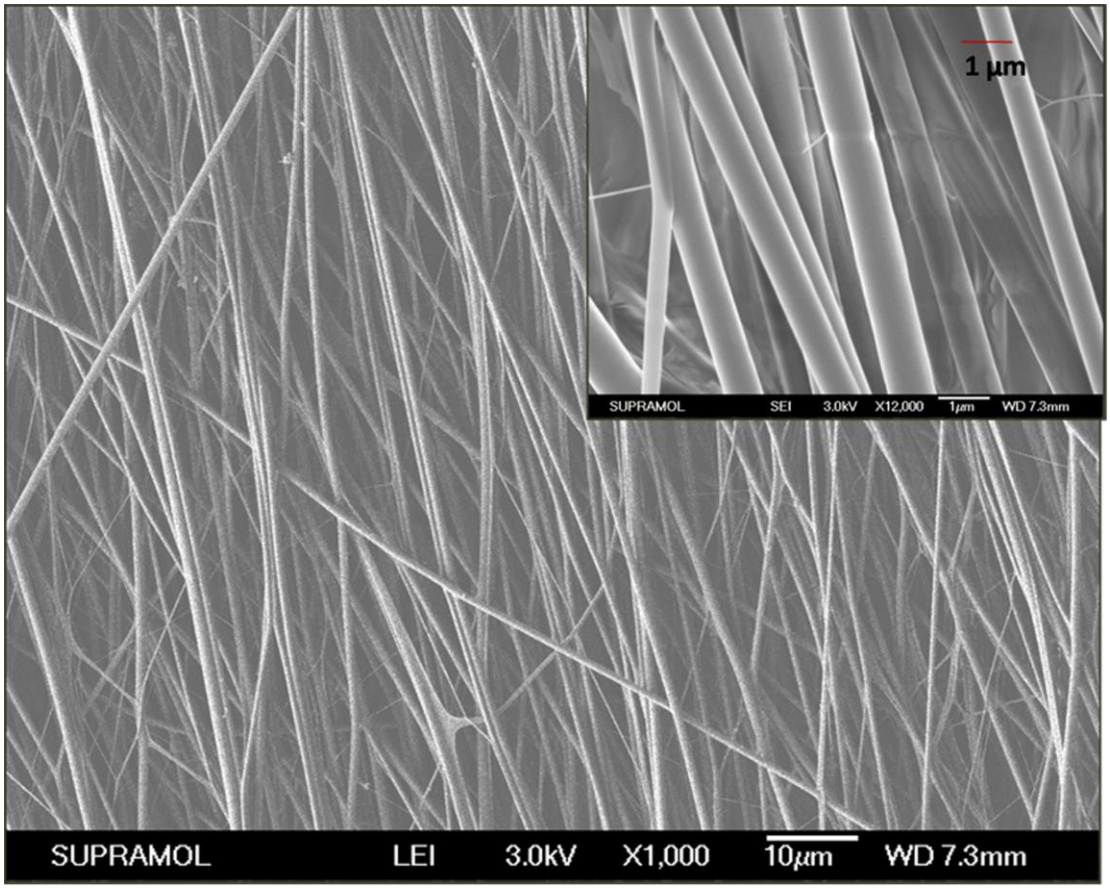

Figure 2. SEM of aligned fibers of G70P30 and the magnification of one segment in the insert figure.

RSC Advances Accepted Manuscript

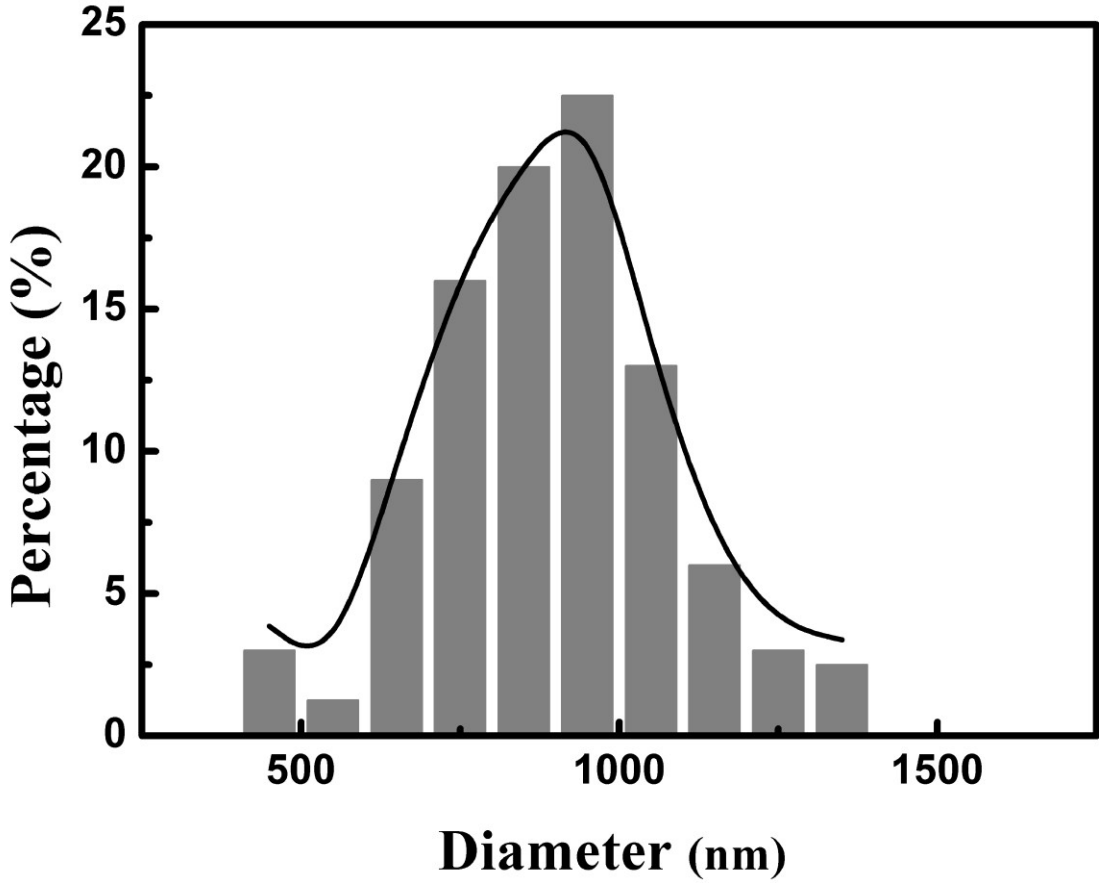

Figure 3. Diameter distribution of aligned fibers of G70PLLA30.

3. Results and Discussion

3.1. Morphology of aligned composite fibrous scaffold

Aligned gelatin/PLLA (G70P30) fibrous membrane with 10 % w/v concentration was made and its morphology was characterized by SEM as shown in Figure 2. As can be seen in Figure 2, the fibers were straight and smooth, and they arranged approximately in single orientation. The diameter mainly distributed between 750-1000 nm as was shown in Figure 3.

RSC Advances Accepted Manuscript

Figure 4. Restorative process of the corneal transparency of NZWRs for 32 weeks postoperative by slit-lamp examination.

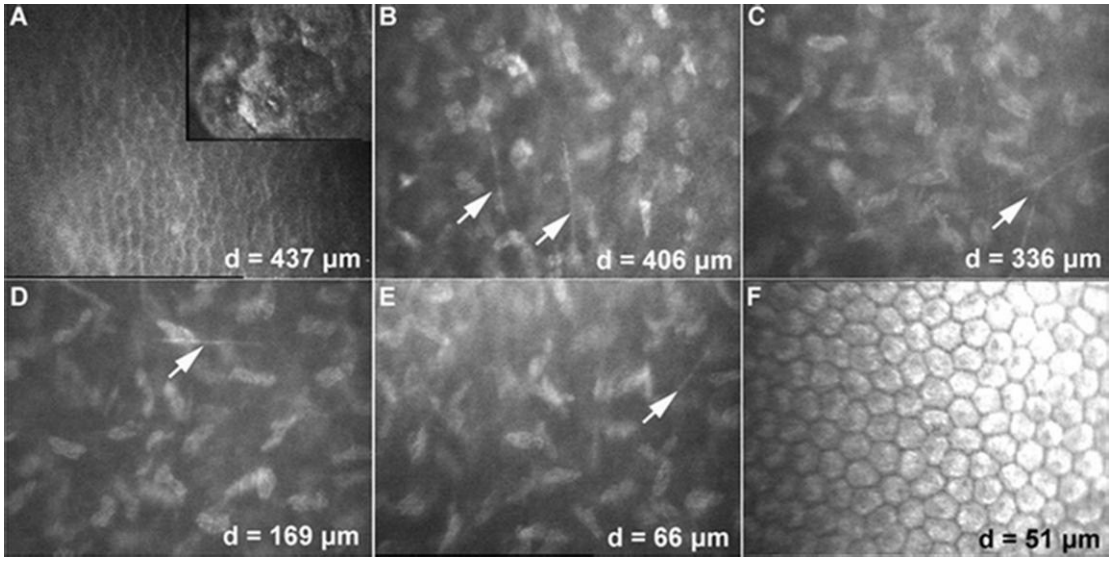

Figure 5. Typical in vivo confocal images of the central cornea of NZWRs for 32 weeks postoperative (A-F). (A) basal epithelial cornea, the innermost epithelial layer; inset of (A) squamous cell of epithelial cornea; (B) anterior stroma; (C, D) middle depth of stroma; (E) posterior stroma; (F) endothelial cornea which is a single layer in the posterior cornea. A confocal image of superficial epithelial cornea, the outermost epithelial layer, is shown in the inset of (A). The arrows mark the nerve fibers.

RSC Advances Accepted Manuscript

3.2. Apparent evaluation of biocompatibility

The biocompatibility of the scaffold was evaluated by observing the scaffold implanted in the eye of NZWRs .The results observed with slit lamp in Figure 4 showed that the fibrous scaffold implanted into the corneal stroma layer presented semitransparent gel state at the first hour (0 days). Two weeks later, it had an observable improvement in transparency. But the transparency declined slightly at the 6th week because of its shrinkage. At the 12th week, the scaffold decrease apparently and became more transparent. At the 24th week, the scaffold became hard to be distinguished from normal cornea and the whole cornea was almost completely transparent at the 32nd week. This showed that the uniaxially aligned fibrous scaffold has good compatibility with cornea. According to the report,[18,19] stylolite could cause the neogenesis of new vessels. From Figure 4, a small amount of new blood vessels had generated around the seams after the 2nd week, but gradually reduced in later observation until they completely disappeared at the 32nd week. Therefore, it could be suggested that the scaffold could not cause the generating of new vessels, which was favorable for the repair of rabbit corneal stroma.

The in vivo confocal images of the allopelagic central cornea of NZWRs for 32 weeks postoperative in Figure 5 showed that nerve fibers (marked by the arrows) were growing in stroma layer of different depth, which indicated that the scaffold could supply some functions for cornea regenerating. All the adjacent keratocytes have normal phenotype, namely an evenly rank of cell and short rod-like cell nucleus. The wing-like

RSC Advances Accepted Manuscript

epithelial and basal cell layers were clearly visible. And the endothelial cells with uniform size and regular shape of hexagon arranged very closely. Table 1 was the statistics analysis of corneal cell densities of different central cornea layers. It showed that there were no significant differences among different central corneal layers in cell density. These results indicated that the implanted aligned fibrous scaffold had no toxic effect on the surrounding tissues.

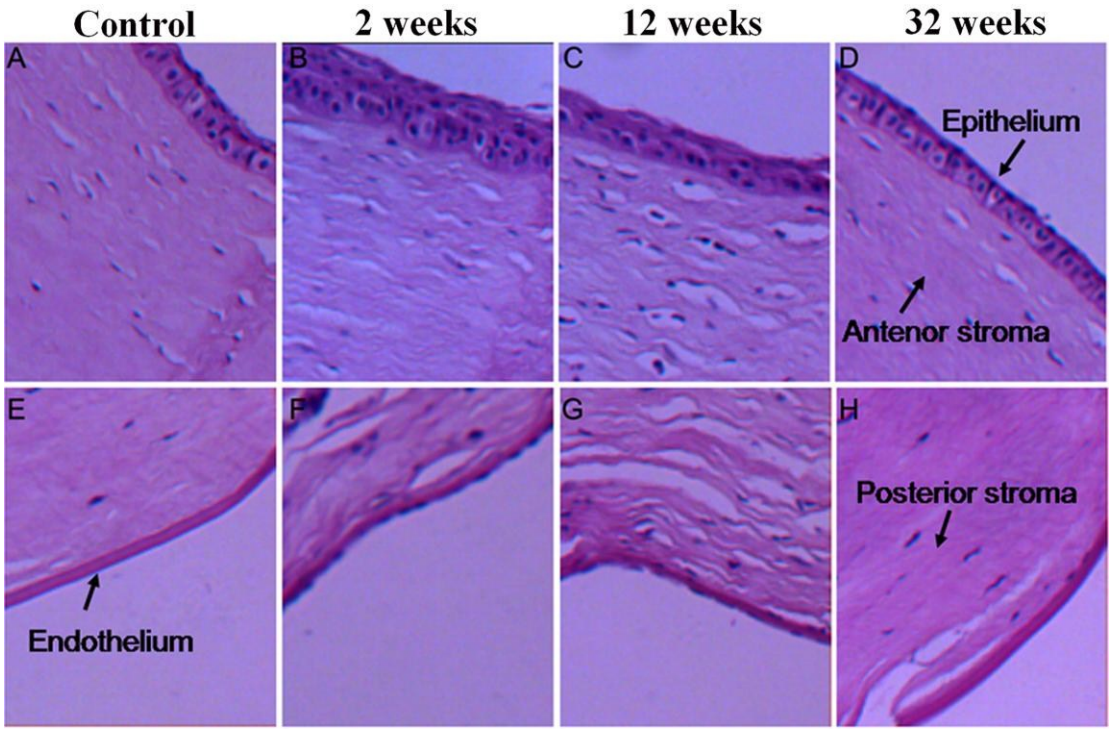

Figure 6. Corneal histocompatibility of the aligned scaffold by HE staining. (A-D) Epithelium and anterior stroma, (E-H) Posterior stroma and endothelium. (A, E) Pre-operative; (B, F) 2 weeks; (C, G) 12 weeks; (F, H) 32 weeks. Magnification: 100×.

RSC Advances Accepted Manuscript

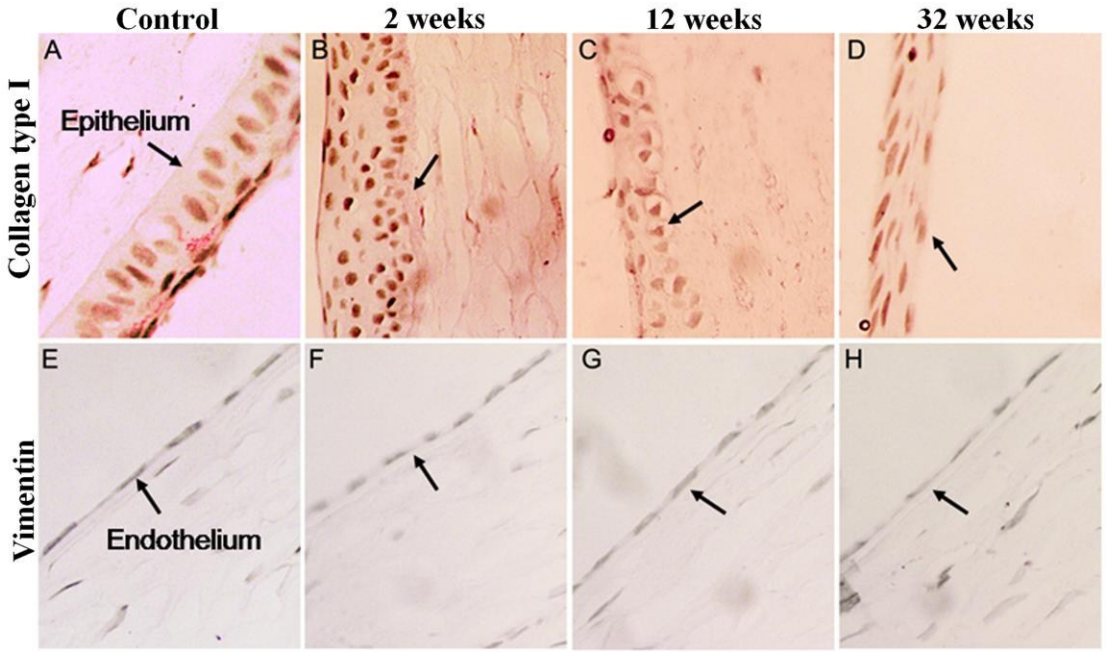

Figure 7. Corneal histocompatibility of scaffolds by immunohistochemical staining. (A-D) are the changes of Epithelium and (E-H) are the changes of Endothelium. (A, E) Preoperative; (B, F) 2 weeks; (C, G) 12 weeks; (F, H) 32 weeks. Magnification: 400×.

The results of HE staining were shown in Figure 6. As can be seen, all the epithelial cells of different periods arranged very closely. The thickness of epithelium layer had increased a little 2 weeks after the operation (Figure 6B), then gradually normalized. (Figure 6C-D).The endothelium was complete with normal thickness (Figure 6E-H). The keratocytes increased in surrounding tissues between the 2nd to the 12th week, and then returned to normal until the 32nd week. The corneal epithelial cells were stained by immunohistochemistry, and the chromogenic results after DAB developing were showed in Figure 7. It was consistent with the result of H&E staining (Figure 6) that the thickness of epithelium increased after the 2nd week. This could be explained that the epithelium

RSC Advances Accepted Manuscript

layer was damaged to some extent during the operation, which might lead to a certain degree of mild edema. The thickness was back to normal at the 12th week through the self-healing process. It's also shown in Figure 7 that endothelium was formed by a single layer of endothelial cells, and there was no obvious change in cell size and arrangement in different periods. These suggested that the implantation of the fibrous scaffold had neither negative effects on the endothelium, nor lesions on surrounding tissues, and this also proved that the scaffold had good histocompatibility.

RSC Advances Accepted Manuscript

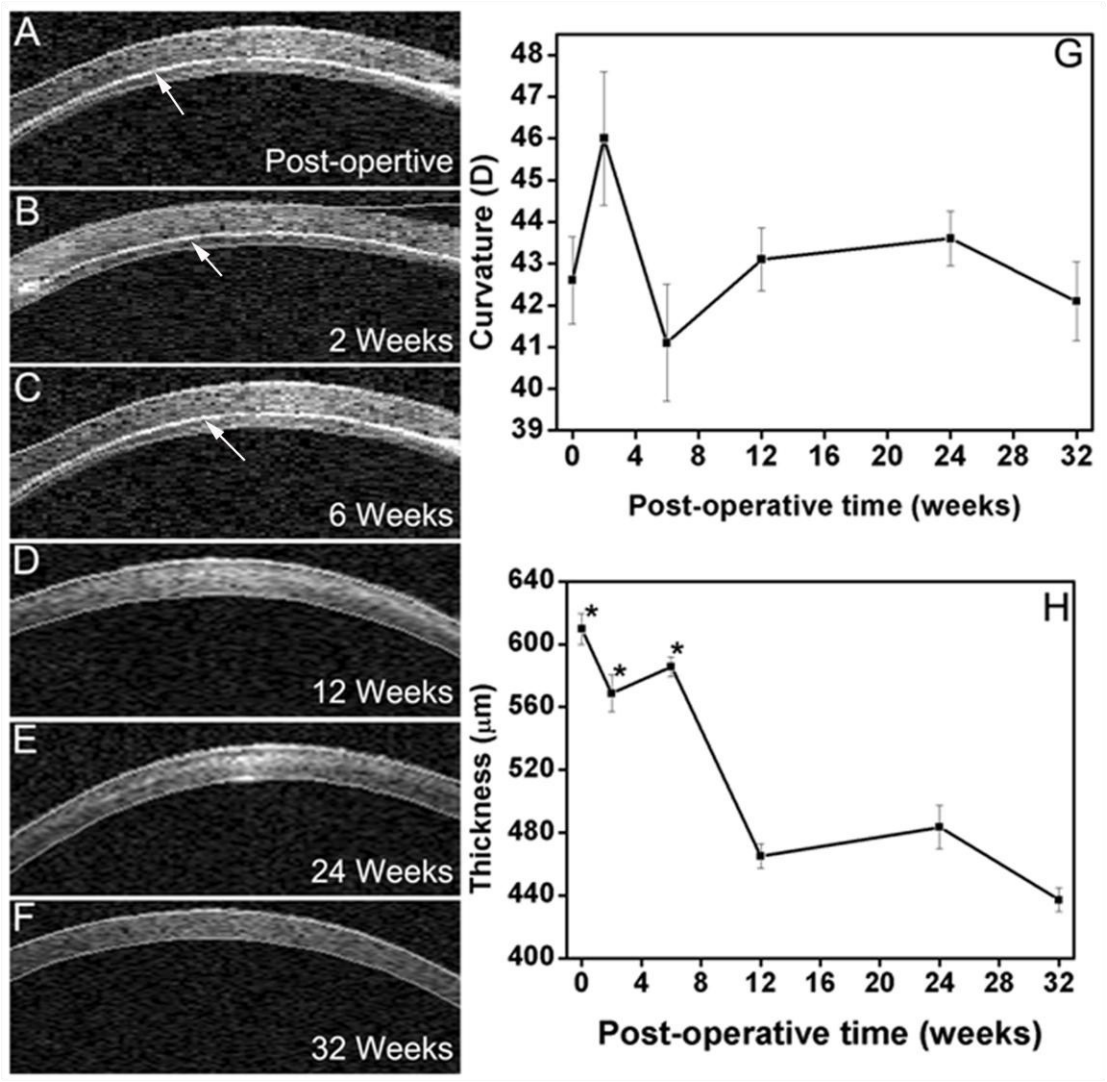

Figure 8. (A-F) Dewarped cross-sectional images of the central cornea of NZWRs for 32 weeks post-operative from optical coherence tomography (OCT) overlaid with detected corneal boundaries; (G) Central corneal curvature; (H) thickness, data are shown in mean ± SD. Arrows mark scaffolds.

3.3. Apparent evaluation of the regeneration process

Anterior segment OCT was used to observe the physiological structure of anterior segment and to measure the thickness and curvature of the cornea for examining the

RSC Advances Accepted Manuscript

regeneration process of the stroma coloboma .The results were shown in Figure 8. The difference in density between the fibrous scaffold and normal corneal tissue led to significant difference in gray level between the scaffold and surrounding tissues in the OCT images. The scaffold was highly reflective as shown in Figure 8A. The scaffold was still distinct at the 6^{th} week. The difference of gray level was blurring after the 12^{th} week and disappeared completely until the 32^{nd} week. The reason was speculated that the scaffold gradually degraded in the observation period and the proliferation of the keratocytes around the scaffold was activated according to the previous pathology characterization. Meanwhile, the scaffold could induce the cells growing into the scaffold gradually to form the extracellular matrix which resulted in the whole density of the scaffold getting increasingly close to that of the surrounding normal tissues.

In addition, Figure 8G showed that there was no significant change in corneal curvature 6 weeks after the operation. Figure 8H showed that the corneal thickness returned to normal gradually 12 weeks after the operation. It indicated that the implanted scaffold had no negative effect on corneal structure which was consistent with the result of the apparent evaluation.

RSC Advances Accepted Manuscript

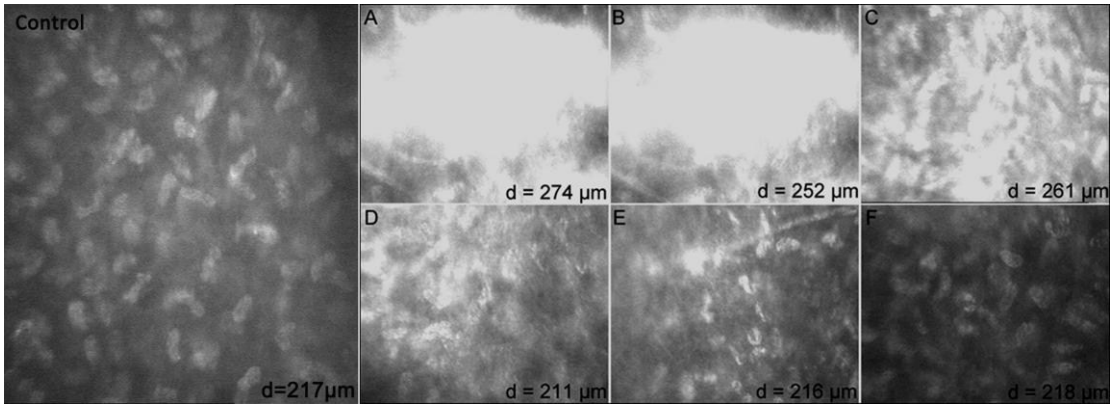

Figure 9. Typical in vivo confocal images of the central cornea of NZWRs at 32 weeks postoperative show the process of cells' ingrowth and tissue regeneration. (A) 0 days. Post-operative; (B) 2 weeks; (C) 6 weeks; (D) 12 weeks; (E) 24 weeks; (F) 32 weeks. The ''d'' value indicates the depth of confocal imaging.

The corneal images of the implant position were obtained by laser scanning confocal microscopy (LSCM) in Figure 9. It showed the migration of stroma cells toward the fibrous scaffold. As can be seen, the scaffold was highly reflective and closely contacted with surrounding tissues in initial postoperative stage (Figure 9A). The cells grew into scaffold gradually during the subsequent observation (Figure 9B-F). The scaffold became non-reflective until the 32nd week. Cells of the central cornea were clearly visible with rod-like nucleus, which had the same phenotype with normal corneal stroma. This changing process was consisted with the results shown in Figure 8, namely, the embedded aligned fibrous scaffold could induce the ingrowth of surrounding keratocytes and keep the normal phenotype of keratocytes. Lamellar structure was formed finally with the increasing amount of keratocytes.

RSC Advances Accepted Manuscript

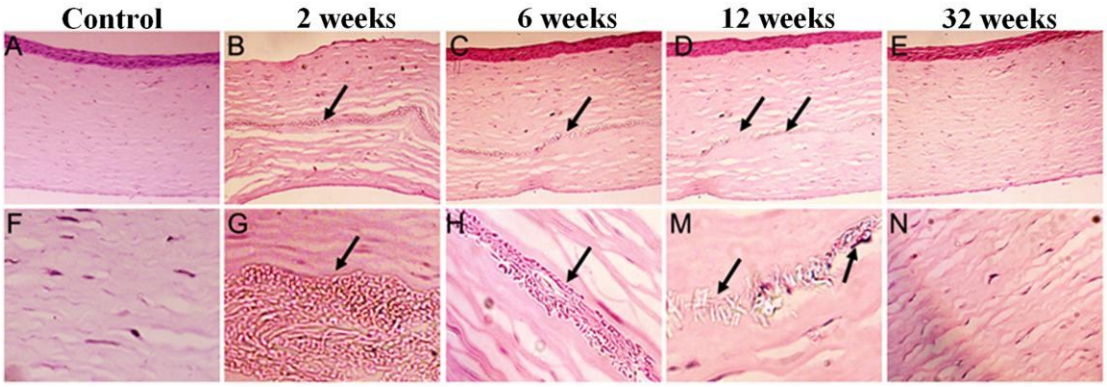

Figure 10. Restorative process of the corneal stroma of NZWRs by HE staining. (A, F) Postoperative, (B, G) 2 weeks, (C, H) 6 weeks, (D, M) 12 weeks,（E, N) 32weeks. Arrows mark scaffolds.

3.4. Pathology evaluation of the regeneration process

It was proved by over apparent evaluation that the uniaxially aligned fibrous scaffold could induce the ingrowth of surrounding keratocytes and keep their normal phenotype. In this section, the ingrowing process and the forming process of collagen type I fibers were further confirmed by tissue section staining. The results of HE staining were shown in Figure 10. Figure 10A and Figure 10F were preoperative contrast figures. By comparison, the scaffold was clearly discernible at the 2nd week postoperative, and had begun to heal over with the surrounding tissues between the 6th and the 12th week. Then the scaffold completely disappeared and entirely normal tissues were formed until the 32nd week. Zoomed-in images in Figure 10F-N revealed the in-growing process more clearly.

RSC Advances Accepted Manuscript

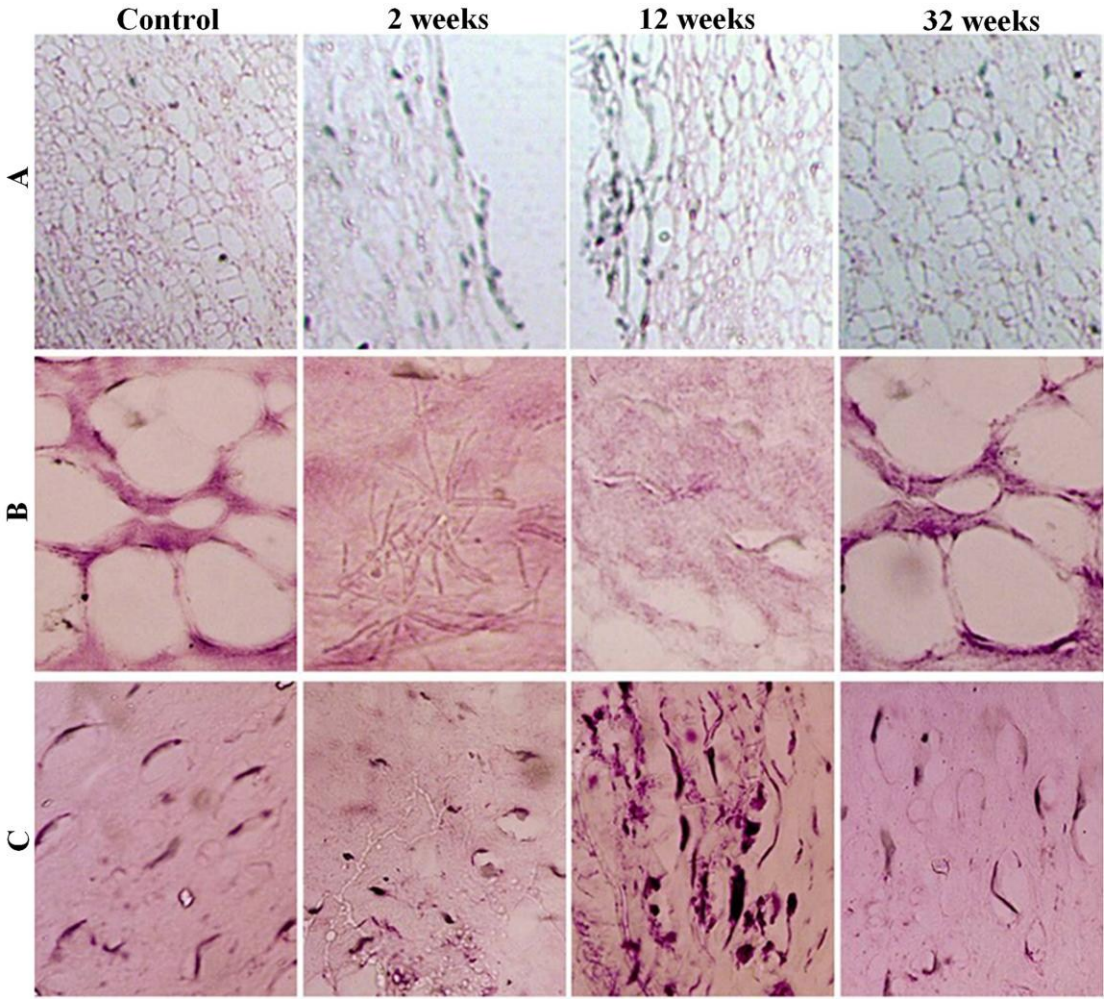

Figure 11. Restorative process of the corneal stroma of NZWRs by immunohistochemical staining of (A) both collagen type I and Vimentin, (B) collagen type I, (C) Vimentin. Magnification: (A) 200×, (B) 400×, (C) 200×.

Immunohistochemical staining results were shown in Fig.11. It was can be seen in Fig.11 that the structure of collagen fibers had normalized gradually after the operation Figure.11A, and the keratocytes of new tissues could be expressed by specific protein—vimentin Figure 11B. This structure of the regenerated corneal stroma composed of parallel aligned collagen fibers and orderly arranged keratocytes played an important role in keeping the corneal transparency.[20,21]

RSC Advances Accepted Manuscript

3.5. Mechanism of in situ induction and repairing

According to the experimental results above, the repair mechanism of *in situ* induction of uniaxially aligned composite fibrous scaffold to rabbit corneal stroma can be speculated as follows.

In the first period, the scaffold provided the necessary condition for cell living, activation and proliferation of keratocytes from surrounding tissues. The activated keratocytes were the cell source for *in situ* regeneration. In this way, immunological rejection of foreign cells was avoided. Besides, the good histocompatibility of scaffold made the scaffold closely connect with surrounding tissues, which would stimulate the ingrowth of activated keratocytes.

In the medium term, the uniaxially aligned arrangement of fibers in the scaffold inducted the keratocytes to arrange in parallel and kept their polarized growth until the repair was completed. And this character was essential for maintaining the corneal transparency.[22-24] Because of the proper porous structure of the fibrous scaffold, it admitted the ingrowth of adequate cells to form three-dimensional structure.[25-27]

During the medium to the last period, the corneal keratocytes grown into the scaffold formed normal cellular phenotype and physiological function. On the other hand, uniaxially aligned scaffold disappeared because of degradation, which would ensure the collagen fibers arranged easily without physical obstacles.

RSC Advances Accepted Manuscript

Conclusion

The uniaxially aligned composite scaffold had good consistency with corneal tissues, and this provided basic security assurance for the successful repair of the corneal stroma. The evaluation results of apparent and pathology during the repair process showed that the implanted scaffold could induct the ingrowth of corneal keratocytes and keep their normal physiological function, and this provided the possibility of promoting the formation of new tissues. The composite scaffold could provide the three-dimensional space for cell growing and induced autologous cells to form normal cellular phenotype and physiological structure.

Acknowledgement

This work was supported by the National Natural Science Foundation of China (Nos. 21104023) and the Key Program of the Science and Technology Department of Jilin Province, PR China (No. 20140204053GX).

RSC Advances Accepted Manuscript

Notes and References

1. S. Salehi, M. Fathi, S. H. Javanmard, T. Bahners, J. S. Gutmann, S. Ergün, K. P. Steuhl and T. A. Fuchsluger, *Macromol. Mater. Eng.*, 2014, **299**, 455.
2. H. J. Levis, I. Massie, M. A. Dziasko, A. Kaasi and J. T. Daniels, *Biomaterials*, 2013, **34**, 8860.
3. S. Salehi, T. Bahners, J. S. Gutmann, S. L. Gao, E. Mäder, and T. A. Fuchsluger, *RSC Adv.*, **4**, 16951.
4. B. J. Klenkler, D. Dwivedi, J. A. West-Mays and H. Sheardown, *J. Biomed. Mater. Res.* A, 2010, **93**, 1043.
5. L. N. Guan, P. Tian, H. Y. Ge, X. L. Tang, H. Zhang, L. L. Du and P. Liu, *J. Mol. Hist.*, 2013, **44**, 609.
6. H. L. Luo, Y. B. Lu, T. T Wu, M. Zhang, Y. J. Zhang and Y. Jin, *Biomaterials*, 2013, **34**, 6748.
7. R. Sakai, B. John, M. Okamoto, J. V. Seppälä, J. Vaithilingam, H. Hussein and R. Goodridge, *Macromol. Mater. Eng.*, 2013, **298**, 45.
8. J. Y. Lai, *RSC Adv.*, 2014, **4**, 18871.
9. J. Wu, Y. Q. Du, M. M. Mann, J. L. Funderburgh and W. R. Wagner, *Exp. Eye. Res.*, 2014, **120**, 71.
10. S. Koo, R. Muhammad, G. S. Peh, J. S. Mehta and E. K. Yim, *Acta Biomater.*, 2014, **10**, 1975.
11. N. A. Ghafar, K. H. Chua, W. Z. W. Ngah, J. C. Hamzah, F. Othman, R. A. Rahman

RSC Advances Accepted Manuscript

and R. H. Idrus, *Cell Tissue Bank*, 2014, **15**, 25.

12. M. Alaminos, M. D. C. Sánchez-Quevedo, J. I. Muñoz-Ávila, D. Serrano, S. Medialdea, I. Carreras and A. Campos, *Invest. Ophthalmol. Vis. Sci*,. 2006, 47, 3311.
13. N. E. Vrana, N. Builles, V. Justin, J. Bednarz, G. Pellegrini, B. Ferrari, O. Damour, D. J. S. Hulmes and V. Hasirci, *Invest. Ophthalmol. Vis. Sci.* 2008, **49**, 5325.
14. R. Lanza, R. Langer and J. P. Vacanti, Principles of tissue engineering. *Academic Press*, 2011.
15. D. Duan, B. J. Klenkler and H. Sheardown, *Expert. Rev. Med. Devices*, 2006, **3**, 59.
16. J. Yan, L. H. Qiang, Y. Gao , X. J. Cui, H. Y. Zhou, S. L. Zhong, Q. Wang and H. Y. Wang, *J. Biomed. Mater. Res. A*, 2012, **100**, 527.
17. Y. Gao, J. Yan, X. J. Cui, H. Y. Wang and Q. Wang, *Chem. Res. Chinese Universities*, 2012, **28**, 1022.
18. B. Ozcelik, K. D. Brown, A. Blencowe, M. Daniell, G. W. Stevens and G. G. Qiao, *Acta Biomaterialia*, 2013, **9**, 6594.
19. J. Zavala, G. R. L. Jaime, C. A. R. Barrientos and J. Valdez-Garcia, *Eye*, 2013, **27**, 579.
20. N. Builles, H. Janin-Manificat, M. Malbouyres, V. Justin, M. R. Rovère, G. Pellegrini, J. Torbet, D. J. S. Hulmes, C. Burillon, O. Damour and F. Ruggiero, *Biomaterials*, 2010, **31**, 8313.
21. T. J. Duncan, Y. Tanaka, D. Shi, A. Kubota, A. J. Quantock and K. Nishida, *Biomaterials*, 2010, **31**, 8996.

RSC Advances Accepted Manuscript

22. S. Salehi, M. Fathi, S. H. Javanmard, T. Bahners, J. S. Gutmann, S. Ergün, K. P. Steuhl and T. A. Fuchsluger, *Macromol. Mater. Eng.*, 2013, **299**, 455.

23. K. Tonsomboon, M. L. Oyen and *J. Mech. Behav. Biomed. Mater.*, 2013, **21**, 185.

24. B. D. Lawrence, J. K. Marchant, M. A. Pindrus, F. G. Omenetto and D. L. Kaplan, *Biomaterials*, 2009, **30**, 1299.

25. W. G. Liu, C. Deng, C. R. McLaughlin, P. Fagerholm, N. S. Lagali, B. Heyne, J. C. Scaiano, M. A. Watsky, Y. Kato, R. Munger, N. Shinozaki and F. F. Li and M. Griffith, *Biomaterials*, 2009, **30**, 1551.

26. M. Rafat, F. Li, P. Fagerholm, N. S. Lagali, M. A. Watsky, R. Munger, T. Matsuura and M. Griffith, *Biomaterials*, 2008, **29**, 3960.

27. C. R. McLaughlin, M. C. Acosta, C. Luna, W. G. Liu, C. Belmonte, M. Griffith and J. Gallar, *Biomaterials*, 2010, **31**, 2770.

RSC Advances Accepted Manuscript

Table 1. Corneal cell densities of different central cornea layers.

Cell density (cells/mm^2)	Epithelium	Anterior stroma	Posterior stroma	Endothelium
Control	4827±156	897±143	465±158	2502±191
32weeks	4736±145	927±197	486±137	2473±177

RSC Advances Accepted Manuscript